Bacteria-induced mixing in natural waters

Originally published in:
Geophysical Research Letters 44(18), https://doi.org/10.1002/2017GL074868

AGU PUBLICATIONS

Geophysical Research Letters

RESEARCH LETTER
10.1002/2017GL074868

Key Points:
- We report the first observation and quantification of bacteria-induced mixing in a stratified natural water body
- The observed mixed layer is 0.3 to 1.2 m thick and located at 12 m depth in an Alpine Swiss Lake
- Bioconvection may be a common but overseen phenomenon in natural waters and relevant in algal bloom dynamics.

Supporting Information:
- Supporting Information S1
- Movie S1

Correspondence to:
T. Sommer,
tobias.sommer@hslu.ch

Citation:
Sommer, T., et al. (2017), Bacteria-induced mixing in natural waters, *Geophys. Res. Lett.*, *44*, 9424–9432, doi:10.1002/2017GL074868.

Received 11 JUL 2017
Accepted 14 AUG 2017
Accepted article online 24 AUG 2017
Published online 22 SEP 2017

Bacteria-induced mixing in natural waters

T. Sommer[1], F. Danza[2,3], J. Berg[4], A. Sengupta[5], G. Constantinescu[6], T. Tokyay[7], H. Bürgmann[1], Y. Dressler[8], O. Sepúlveda Steiner[8], C. J. Schubert[1], M. Tonolla[2,3], and A. Wüest[1,8]

[1]Department of Surface Waters - Research and Management, Eawag, Kastanienbaum, Switzerland, [2]Department for Environment Constructions and Design (DACD), Laboratory of Applied Microbiology (LMA), University of Applied Sciences and Arts of Southern Switzerland (SUPSI), Bellinzona, Switzerland, [3]Department of Botany and Plant Biology, University of Geneva, Geneva, Switzerland, [4]Department of Biogeochemistry, Max Planck Institute for Marine Microbiology, Bremen, Germany, [5]Department of Civil, Environmental and Geomatic Engineering, Institute of Environmental Engineering ETH Zurich, Zurich, Switzerland, [6]Department of Civil and Environmental Engineering, University of Iowa, Iowa City, USA, [7]Department of Civil Engineering, Middle East Technical University, Ankara, Turkey, [8]Physics of Aquatic Systems Laboratory, Margaretha Kamprad Chair, EPFL-ENAC-IEE-APHYS, Lausanne, Switzerland

Abstract Swimming organisms can enhance mixing in their natural environments by creating eddies in their wake and by dragging water along. However, these mixing mechanisms are inefficient for microorganisms, because swimming-induced variations in velocity, temperature, and dissolved substances are evened out before they can be advected. In bioconvection, however, microorganisms induce water movement not by propulsion directly but by locally changing the fluid density, which drives convection. Observations of bioconvection have so far mainly been limited to laboratory settings. We report the first observation and quantification of bioconvection within a stratified natural water body. Using in situ measurements, laboratory experiments, and numerical simulations, we demonstrate that the bacterium *Chromatium okenii* is capable of mixing 0.3 to 1.2 m thick water layers at around 12 m water depth in the Alpine Lake Cadagno (Switzerland). As many species are capable of driving bioconvection, this phenomenon potentially plays a role in species distributions and influences large-scale phenomena like algal blooms.

Plain Language Summary Small aquatic organisms (length $< \approx 1$ cm) do not efficiently mix water by swimming, because they are too small and swim too slowly to create whirls that lead to mixing. In bioconvection, however, small organisms (that are denser than water and, on average, swim upward) can mix water. When such organisms accumulate locally in a layer, the density of the water increases. This layer of heavier water on top of lighter water sinks and mixes with the surrounding water. Continuous upward swimming provides the energy to maintain the water motion. Bioconvective mixing has been observed for a wide range of species, but so far mainly in the laboratory. We report the first observation of bioconvection in a natural water body and show that the only 10 μm long bacterium *Chromatium okenii* causes mixing in the Alpine Lake Cadagno (Switzerland). The observed mixed layer is 0.3 to 1.2 m thick and located at around 12 m depth. We suggest that bioconvection may influence the composition of organisms in natural waters and affect large-scale phenomena like algal blooms.

1. Introduction

Whether or not swimming organisms significantly contribute to mixing in oceans and inland water bodies has long been debated [*Kunze et al.*, 2006; *Visser*, 2007; *Gregg and Horne*, 2009; *Katija and Dabiri*, 2009; *Kunze*, 2011; *Katija*, 2012]. This debate mainly focuses on the concept of propulsion-induced mixing where a swimming organism creates small-scale eddies that bring different water masses into contact with one another. Molecular diffusion then occurs between those water masses.

For microorganisms, however, viscosity inhibits the creation of eddies. Moreover, molecular diffusion evens out variations in temperature and dissolved substances before they are dragged along. For the most prevalent inhabitants of natural water bodies by numbers and biomass—bacteria, phytoplankton, and copepods—propulsion-based mixing is thus negligible [*Visser*, 2007; *Kunze*, 2011].

Nevertheless, small organisms can cause mixing by a different mechanism: bioconvection [*Pedley and Kessler*, 1992b; *Hill and Pedley*, 2005]. Microorganisms can trigger bioconvection, if they are denser than water and

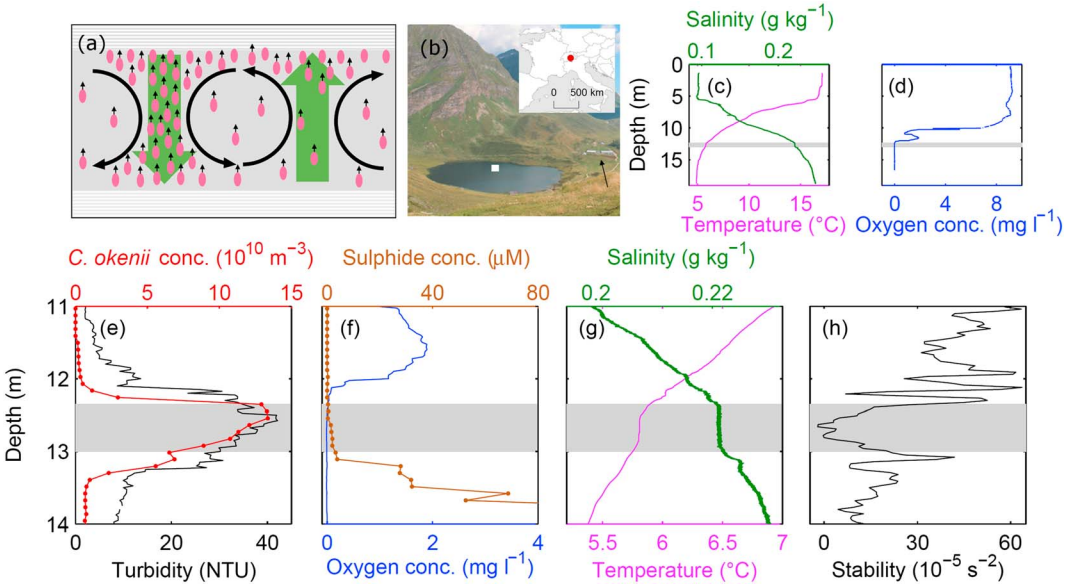

Figure 1. Co-occurrence of the mixed layer and the layer of maximum abundance of *C. okenii* in Lake Cadagno. (a) Schematic of bioconvection (side view). The microorganisms (magenta ellipsoids) located in the bioconvective layer (grey area) are continuously swimming upward (indicated by upward arrows). At the top of the layer, they stop swimming upward and cells accumulate. Large cell concentrations increase the local water density and form sinking plumes (green downward arrow), whereas lower cell concentrations are found in the upward plumes (green upward arrow). Circular convective currents (long black curved arrows) are formed by alternating sinking and rising plumes. (b) Photograph of Lake Cadagno, sampling site (indicated by white square), laboratory buildings (indicated by black arrow), and its location within Europe (inset, data source: swisstopo (Art. 30 GeoIV): 5704 000 000/DHM25@2003, reproduced with permission of swisstopo/JA100119). (c) Temperature and salinity profiles measured on 5 August 2015 at 09:00 hours with the vertical microstructure profiler (VMP-500). The grey shading indicates the depth interval of the mixed layer and is repeated in Figures 1d–1h. (d) Oxygen profile measured with a Sea & Sun CTD. (e) *C. okenii* concentration (measured by flow cytometry) and turbidity (measured with a Sea-Bird Scientific CTD) profiles. (f) Zoomed-in oxygen section from Figure 1d and sulphide concentrations measured in the water samples. (g) Zoomed-in temperature and salinity section from Figure 1c. (h) Stability profile calculated from the temperature and salinity measurements in Figure 1c. In Figures 1e and 1f, the turbidity and oxygen profiles were smoothed by a moving average using a depth interval window of 5 cm.

swim upward against gravity, for example, toward light [*Jékely*, 2009], oxygen [*Fenchel and Finlay*, 2008], or because of a stabilizing torque exerted on the cell body by the gravitational force (gravitaxis) [*Lebert and Hader*, 1996; *Sengupta et al.*, 2017]. Both criteria are common for many phytoplankton species, in particular dinoflagellates and raphidophytes [*Kamykowski et al.*, 1992], which are known to form harmful algal blooms [*Smayda*, 2010]. Fluid motions are induced when those microorganisms accumulate locally in a layer, which is a common phenomenon in nature [*Durham and Stocker*, 2012], and thereby increase its density. This layer of heavier water on top of lighter water eventually becomes unstable and breaks up into characteristic plumes, initiating bioconvective mixing (see schematic in Figure 1a). The plumes are faster than the swimming speed of the microorganisms [*Pedley and Kessler*, 1992a], and the organisms are thus dragged along with the plumes. However, active upward swimming relative to the plumes is required to continuously supply potential energy and maintain convective mixing.

Barring a report of zooplankton "micropatches" observed on the surface of the Baltic Sea [*Kils*, 1993] and patterns observed on the surface of an intertidal tide pool [*Bearon and Grünbaum*, 2006, Figure 3], bioconvection has so far been limited to laboratory observations and its relevance to natural aquatic systems has remained unclear [*Jánosi et al.*, 2002].

In this study, we demonstrate that bacteria cause mixing within a natural water body. Biological and chemical analysis of water column samples and high-resolution temperature and salinity profiles, taken over three summer seasons in Lake Cadagno, Switzerland, revealed that mixing occurred consistently at a water depth between 10 m and 15 m, where a population of the motile purple sulphur bacterium *Chromatium okenii* (*C. okenii*) was located. Our measurements of *C. okenii* concentrations, density, swimming speed, and water density were then used as input parameters for direct numerical simulations, which successfully reproduced the mixed layer thicknesses and energy dissipation rates obtained from in situ measurements taken in the lake.

2. Materials and Methods

2.1. Water Sampling

All measurements were taken from a float fixed at the deepest point of Lake Cadagno (46.55087°N, 8.71153°E, water depth ~ 21 m, 1920 m asl). Water for analysis was pumped to the surface through a Tygon® tube (20 m long, inner diameter 6.5 mm, volume 0.66 L) at a flow rate of 1 L min^{-1} using a peristaltic pump (Cole-Parmer Instrument Co., USA, Universal Electric Co., USA). Before sampling, 1 L of water was pumped up and discarded to refill the tubing with water from the desired sampling depth. The tube inlet, which was suitable for high-resolution depth sampling [*Jorgensen et al*., 1979], was placed directly in front of a Sea-Bird Scientific CTD-type SBE 19plus V2, which enabled us to match the physical profiles to the depths of the water samples. The CTD was lowered together with the tubing at 5 cm s^{-1}, sampling at 4 Hz, to a depth of approximately 1 m above the layer of maximum *C. okenii* concentration. From there onward, we sampled at depths of every 10 cm, such that within 30 to 40 sampling counts, we spanned the entire *C. okenii* layer, including its surroundings above and below.

2.2. Sulphide, Turbidity, and Oxygen Measurements

Sulphide concentrations were measured photometrically using the methylene blue method [*Cline*, 1969]. Turbidity was measured with a Sea-Bird Scientific WET Labs (USA) ECO NTU turbidity sensor attached to a Sea-Bird Scientific CTD. The sensor operates at a wavelength of 700 nm and has a sensitivity of 0.02 NTU. Oxygen (mg L^{-1}) was measured with an OxyGuard Ocean Probe (Denmark) mounted on the Sea & Sun (Germany) CTM281 multiparameter probe (sampling at 2.4 Hz), which was lowered together with the Sea-Bird CTD. The response time and the resolution of the oxygen probe is approximately 10 s and 0.1 mg L^{-1}, respectively. The oxygen signal of the probe was calibrated against water samples taken at the surface and at a depth of 14 m; the samples were analyzed for oxygen using Winkler titration.

2.3. *C. okenii* Concentration

Cell concentrations (m^{-3}) were measured in unstained samples (50 μL) using flow cytometry [*Casamayor et al*., 2007]. We used a BD Accuri C6 cytometer (Becton Dickinson, USA) at a flow rate of 66 μL min^{-1}, equipped with two lasers (emitting at wavelengths of 488 nm and 640 nm, respectively), two scatter detectors, and four fluorescence detectors (laser 488 nm: FL1 = 533/30, FL2 = 585/40, and FL3 = 670 LP; laser 640 nm: FL4 = 670). The data were analyzed with the BD Accuri C6 Software (v. 1.0.264.21; Becton Dickinson, USA) by thresholding first the forward scatter (FSC-H $>$ 10,000) to exclude debris and abiotic particles and subsequently the FL3 filter (FL3-A $>$ 1,100), to select living cells with natural fluorescence of chlorophyll and bacteriochlorophyll (Figure S1a in the supporting information). The population of the photosynthetic large-celled purple sulphur bacterium *C. okenii* was reliably distinguished from other photosynthetic sulphur bacteria, enabling us to define a gate for enumeration around the tight cluster with high side scatter (SSC) and forward scatter (FSC) in an SSC versus FSC scatterplot (Figure S1b). The percentage of *C. okenii* over the total population was determined by dividing the counts of *C. okenii* (red circle in Figure S1b) by the total counts (the integrated counts shown in Figure S1a).

2.4. Temperature and Conductivity Profiles

High-resolution profiles of temperature and conductivity were measured [*Sommer et al*., 2013] with a loosely tethered, free-falling Vertical Microstructure Profiler (VMP-500, Rockland Scientific International, RSI, Canada), adjusted to a profiling speed of 0.07 to 0.1 m s^{-1}, at a sampling rate of 512 Hz. Two fast FP07 (RSI, Canada and GE, USA) thermistors (5 cm apart from each other) and two fast SBE-7 (Sea-Bird Scientific, USA) conductivity microsensors (2.6 cm apart) were mounted at the tip of the instrument. The time response of the thermistors has a half-power frequency of 10.2 Hz and a root-mean-square (RMS) noise level of 1.2×10^{-5} K. At small profiling speeds $<$0.19 m s^{-1}, the response of the conductivity sensors is dominated by the spatial response caused by the finite measurement volume and has a half-power wave number of $240 \times 2\pi$ rad m^{-1}. The RMS noise levels of the two conductivity sensors are 0.12 μS cm^{-1} and 0.06 μS cm^{-1}, respectively [*Sommer et al*., 2013]. To increase the absolute accuracy, the microstructure signals were calibrated against the CTD temperature and conductivity signals of a Sea-Bird SBE-4C (initial accuracy and drift per year less than 1 μS cm^{-1}, based on long-term experience from our lab) and SBE-3F sensors (initial accuracy and drift

Table 1. Measured Parameters of the *C. okenii* Layer[a]

Parameter Measured	Units	Measurement Date: August 2014	June 2015	August 2015	September 2015	July 2016
Thickness of mixed layer (H_{ml})	m	**1.2** ± 0.4 (23)	n.d.	**0.3** ± 0.2 (21)	n.d.	**0.9** ± 0.3 (13)
Stability in mixed layer (N^2_{ml})	10^{-5} s^{-2}	**0.4** ± 0.2 (23)	n.d.	**1.6** ± 2.2 (21)	n.d.	**0.2** ± 0.3 (13)
Stability of background water stratification (N^2_{bulk})	10^{-5} s^{-2}	**8.7** ± 2.2 (23)	**26**.3 ± 4.1 (8)	**28.4** ± 4.2 (21)	**34.5** ± 16.8 (4)	**7.9** ± 2.0 (13)
Dissipation rate in mixed layer (ε_{ml})	10^{-10} W kg^{-1}	**3.6** ± 3.7 (45)	n.d.	**3.7** ± 2.6 (42)	n.d.	**3.4** ± 2.1 (24)
Dissipation rate below mixed layer (ε_{bel})	10^{-10} W kg^{-1}	**0.8** ± 1.4 (42)	n.d.	**2.5** ± 1.8 (39)	n.d.	**1.7** ± 2.1 (23)
Background corrected dissipation rate ($\varepsilon_{ml} - \varepsilon_{bel}$)	10^{-10} W kg^{-1}	**2.9** ± 4.4 (41)	n.d.	**1.1** ± 3.0 (39)	n.d.	**1.7** ± 3.7 (22)
Concentration of *C. okenii* in the *C. okenii* layer (C_B)	10^{10} m^{-3}	**11.6** ± 1.4 (5)	**3.9** ± 1.3 (6)	**7.5** ± 2.8 (90)	**1.1** ± 0.4 (20)	**13.9** ± 5.3 (6)
Ratio of *C. okenii* cells over all cells in the *C. okenii* layer	%	**16** ± 2 (5)	**7** ± 2 (6)	**5** ± 2 (90)	**2** ± 1 (20)	**12** ± 4 (6)
Thickness of *C. okenii* layer (H_B)	m	**2.0** (1)	**0.2** ± 0.2 (3)	**0.6** ± 0.3 (12)	**1.0** ± 0.3 (2)	**1.0** (1)

[a]Shown are arithmetic mean values (bold) ± standard deviation followed by the number of samples in brackets (n.d. signifies not determined). The measurements of August 2015, which are used in the numerical simulation, are highlighted in grey.

per year of 1 mK), respectively, using a second order polynomial fit. These SBE sensors were also mounted close to the microsensors on the VMP-500 and sampled at 64 Hz.

2.5. Salinity, Density, and Stability Calculations

Salinity and water density ρ (kg m^{-3}) (without *C. okenii*) were calculated from the microstructure temperature and conductivity data [*Wüest et al.*, 1996] using the characteristic ionic composition of Lake Cadagno water. Depth z was calculated from pressure p (bar) by first subtracting the ambient air pressure and then multiplying by a scaling factor of 10.195 m bar^{-1}. This scaling factor was obtained for an average density profile by linearly fitting z to p, where z was iteratively computed by $z_i = z_{i-1} + \frac{p_i - p_{i-1}}{\rho_i g}$ and i is the iteration number. The vertical density gradient used in the definition of N^2 was determined by linear fits of ρ against z, either within the mixed layer for N^2_{ml} or within a 4 m interval (more than twice the largest mixed layer thickness) for N^2_{bulk}.

2.6. Thickness of the *C. okenii* Layer and the Mixed Layer

The upper and lower boundaries of the *C. okenii* layer were extracted from a cell concentration profile obtained using flow cytometry by selecting the depths, where the *C. okenii* concentration exceeded 50% of the maximum concentration in that profile. The shallowest and deepest selected depths were then used to define the layer boundaries. The mixed layer was identified visually from the temperature and conductivity microstructure profiles by selecting the depth range of homogenous temperature and conductivity bounded by distinct gradients above and below. Only mixed layers with thicknesses larger than 0.1 m were considered.

3. Results

Our site for the study, Lake Cadagno [*Del Don et al.*, 2001] (Figure 1b), is a small lake in the Swiss Alps (46.55°N, 8.71°E, 1920 m asl maximum depth 21 m, and surface area 0.26 km^2). Lake Cadagno is meromictic, which signifies that the density of the water (a function of temperature and salinity) always increases with depth in the deep part of the lake. During winter, the ion-rich deep water, supplied by subsurface springs, limits the depth of convective surface cooling and keeps the deep water permanently stratified and anoxic [*Del Don et al.*, 2001]. During summer, both, temperature (decreasing with depth from 17°C to 5°C in Figure 1c) and salinity (increasing with depth from 0.1 g kg^{-1} to 0.25 g kg^{-1} in Figure 1c), contribute to the water column stability and oxygen is limited to depths above 12 m (Figure 1d).

Each year after ice melt in May, a layer of *C. okenii*, accompanied by a peak in turbidity (Figure 1e), develops directly below the interface (oxycline) between oxygen containing (oxic) shallow water and deep, anoxic water rich in sulphide [*Tonolla et al.*, 2005] (Figure 1f). Layer thicknesses, H_B, of *C. okenii* are between 0.2 and 2 m (Table 1 and Figure 1e). *C. okenii* gain energy from light-driven sulphide oxidation and rely on the supply of both sulphide from anoxic waters and light from above [*Imhoff*, 2006]. Using flow cytometry analysis, we found that *C. okenii* were present at cell concentrations, C_B, of 10^{10} to 10^{11} m^{-3}, and were most numerous in the peak summer months (Table 1).

Being denser than water and motile, *C. okenii* are capable of driving bioconvection [*Pfennig*, 1962]. By analyzing water samples taken from Lake Cadagno, we obtained the following parameters for *C. okenii* cells. The swimming speed, w_b, was $(2.7 \pm 1.4) \times 10^{-5}$ m s^{-1} (mean ± standard deviation) (Figure S2a and supporting information Text S1 [*Gervais*, 1997; *Vaituzis and Doetsch*, 1969]). The density, ρ_b, was between 1.15×10^3 and 1.27×10^3 kg m^{-3}, thus clearly exceeding the water density of 1×10^3 kg m^{-3} (Figure S3 and supporting information Text S2 [*Guerrero et al.*, 1985]). The cell volume, V_b, was $(2.45 \pm 0.88) \times 10^{-16}$ m^3 (spherocylinders with a length of $(10 \pm 2) \times 10^{-6}$ m and a width of $(6 \pm 1) \times 10^{-6}$ m, Figure S2b and supporting information Text S1). Other organisms (consisting of sulphur-oxidizing and sulphur-reducing bacteria) within the *C. okenii* layer are nonflagellated (except *Lamprocystis roseopersicina*), and their volume is smaller than 0.1×10^{-16} m^3 [*Musat et al.*, 2008]. Because of their large volume, *C. okenii* represent the largest biovolume fraction within the *C. okenii* layer and we thus expect *C. okenii* to be the relevant organism for biogenic mixing processes. The concentration fraction of *C. okenii* within the layer was 16 ± 2%, 5 ± 2%, and 12 ± 4% in August 2014, August 2015, and July 2016, respectively (Table 1). Assuming that the volume of *C. okenii* is on average 25 times larger than the volume of the other organisms, the corresponding layer averaged biovolume fractions of *C. okenii* are 83%, 57%, and 77%, respectively.

In mid- to late summer, a layer of nearly uniform temperature and salinity (Figure 1g) was found to develop below the oxycline. This uniformity is a hallmark of mixing. The mixed layer thicknesses, H_{ml}, were 1.2 ± 0.4 m, 0.3 ± 0.2 m, and 0.9 ± 0.3 m in August 2014, August 2015, and July 2016, respectively (Table 1), and similar characteristics were found in physical profiles measured in 1990 [*Wüest*, 1994]. No mixed layer could be identified in June 2015 and September 2015, when the *C. okenii* were less abundant (Table 1). In order to enable comparison to other water bodies, we define a normalized density gradient by using the common definition of stability, $N^2 = (g/\rho)\,\partial\rho/\partial z$ (s^{-2}). Here g (m s^{-2}) is the gravitational constant, ρ (kg m^{-3}) is the water density (without *C. okenii*), and z (m) is the depth. Within the mixed layer, the stability N^2_{ml} was reduced by more than 1 order of magnitude compared to the background-water stability N^2_{bulk} (Figure 1h and Table 1). Given that (i) the mixed layer and the *C. okenii* layer physically coincide (Figures 1e, 1g, and 1h), (ii) the cell properties of *C. okenii* enable bioconvection, and (iii) *C. okenii* represent the largest biovolume fraction with the mixed layer, we propose that *C. okenii* trigger the mixing.

To test this hypothesis, we conducted direct numerical simulations (Figure 2 and supporting information Text S3 [*Borden et al.*, 2012; *Chang et al.*, 2006; *Ooi et al.*, 2009; *Pierce and Moin*, 2004]). In these simulations, we used the *C. okenii* concentration and the background-water stratification measured in August 2015, which was the field campaign with most measurements of the relevant parameters (Table 1). We simulated *C. okenii* as a concentration field C, which locally increases fluid density by $\rho_B = (\rho_b\text{-}\rho)V_bC$. Swimming was represented by a net upward population speed w_B, relative to the water, imposed on this concentration field for cells located below the oxycline (which is at 1 m depth in Figure 2). In the region above the oxycline, the swimming speed was set to zero. This implies that the upward swimming *C. okenii* accumulate at the top of the *C. okenii* layer, directly below the oxycline, where they increase the water density. Initially, *C. okenii* were homogeneously distributed within a horizontal layer (of thickness H_B and present at a concentration of C_B), located directly below the oxycline. The diffusivity of the *C. okenii* cells was chosen to be 10^{-8} m^2 s^{-1} (supporting information Text S3 [*Kessler*, 1986; *Kim*, 1996; *Bearon and Grünbaum*, 2006]). Water density increased linearly with depth (Figure 2b).

The simulation demonstrates that *C. okenii* induce convective mixing. The input cell parameters, taken from the measurements in Lake Cadagno, were $V_b = 2.45 \times 10^{-16}$ m^3, $\rho_b = 1.15 \times 10^3$ kg m^{-3}, and $w_B = 9 \times 10^{-6}$ m s^{-1} (one third of w_b, which was motivated by laboratory experiments, Figure S2c and supporting information Text S1), and the initial state was defined by $C_B = 7.5 \times 10^{10}$ m^{-3}, $H_B = 0.6$ m, and $N^2_{bulk} = 2.8 \times 10^{-4}$ s^{-2} (Table 1, August 2015). At the beginning of the simulation, the upward swimming *C. okenii* accumulate below the oxycline, where they locally increase the water density. This denser water becomes unstable and triggers bioconvection (Figures 2c and 2d). The convective layer then gradually expands (Figures S4a and S4b) and reaches a thickness of 0.3 m after 10 h (Figures 2e and 2f and Movie S1 in the supporting information), corresponding to the average thickness of 0.3 m measured in August 2015 in Lake Cadagno (Table 1).

Our simulation further shows that the energy supplied by the *C. okenii* explains the mixing observed. Within the *C. okenii* layer, the heavy *C. okenii* cells supply potential energy by moving upward and the energy input

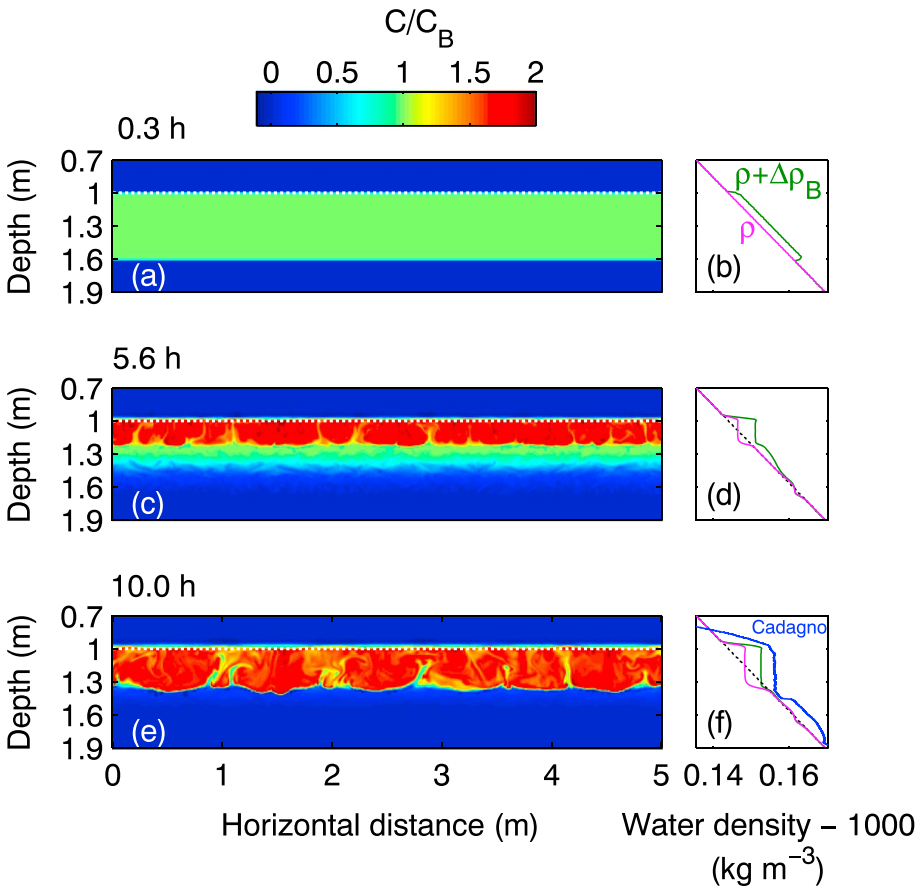

Figure 2. Emergence of a mixed layer in the numerical simulation. (a, c, e) *C. okenii* concentration distributions *C*, normalized by the initial concentration, at three different lapsed times 0.3 h, 5.6 h, and 10.0 h. Only the relevant 0.7 to 1.9 m depth interval out of the 2.6 m high computational domain is shown. (b, d, f) Density profiles as function of depth. Water density without *C. okenii* (ρ) is shown in magenta; water density including *C. okenii* cells ($\rho + \Delta\rho_B$) is shown in green. A density profile (taken on 4 August 2015 at 19:00 hours) from Lake Cadagno is superimposed in blue in Figure 2f. Initially, the *C. okenii* are located in a homogenous layer embedded within a linear density gradient (Figures 2a and 2b). After initializing the simulation, *C. okenii* swim upward and accumulate at the top of the layer below the oxycline (symbolized by the horizontal dotted white line at 1 m depth). There, the water density increases and bioconvection homogenizes the density profile below (Figures 2c and 2d). Within 10 h, the mixed layer expands to a thickness of 0.3 m (Figures 2e and 2f), corresponding to the average mixed-layer thickness of 0.3 m measured in Lake Cadagno in August 2015.

rate, R (W kg^{-1}), is approximated within 10% by $R \approx (g/\rho) w_B (\rho_b - \rho) V_b C_B$ (supporting information Text S4). This energy input of *C. okenii* is converted into an increase of the system's potential energy, dE_p/dt, or it is dissipated into heat by friction. Two more contributions to the energy balance (dE_k/dt and D_V, supporting information Text S4 [*Hieronymus and Carpenter*, 2016; *Winters et al.*, 1995]) were found negligible. At t = 10 h, when the mixed layer thickness in the simulation reached 0.3 m, as measured in Lake Cadagno, the mean dissipation rate ε within the *C. okenii* layer was $(1.0 \pm 1.5) \times 10^{-10}$ W kg^{-1}, or 42% of the bacterial energy input rate $R = 2.4 \times 10^{-10}$ W kg^{-1}. Using the exact definition of R and a longer evaluation period from 10 h to 24 h, the ratio of ε/R was found 45% (Figures S4c and S4d). Within the mixed layer of the simulation, which corresponds to the depth interval evaluated in Lake Cadagno, the mean dissipation rate was $(1.3 \pm 1.4) \times 10^{-10}$ W kg^{-1}, slightly enhanced. In Lake Cadagno, we estimated the dissipation rate ε by analyzing microstructure temperature profiles using the Batchelor fitting method [*Batchelor*, 1959; *Ruddick et al.*, 2000; *Gibson and Schwarz*, 1963; *Steinbuck et al.*, 2009b] (supporting information Text S5). In August 2015, ε in the mixed layer was enhanced by $(1.1 \pm 3.0) \times 10^{-10}$ W kg^{-1} compared to the background water (Figure 3 and Table 1), which matches the ε observed in the simulation (Figure 3c). The dissipation rates measured in the mixed layer of Lake Cadagno can thus be explained by the energy input of *C. okenii*.

Larger energy input rates are expected for microorganisms in other natural settings. For example, we estimate $R \approx 10 \times 10^{-10}$ W kg^{-1} for a population of the dinoflagellate *Gonyaulax polyedra* [*Legović et al.*, 1991;

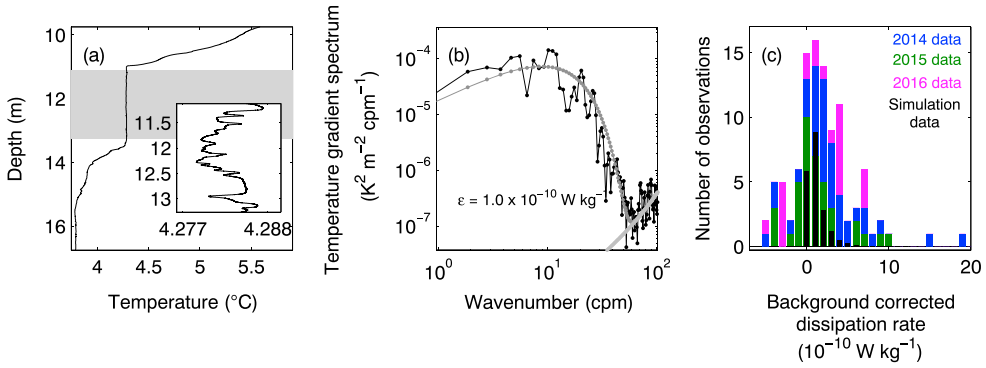

Figure 3. Energy dissipation rates measured in Lake Cadagno are similar to the dissipation rates in the simulation. (a) Temperature section measured in Lake Cadagno (14 August 2014 at 15:00 hours) including the mixed layer (grey shading). The inset in Figure 3a shows an 11 mK zoomed-in window of the mixed-layer temperature that is used in Figure 3b for computing the temperature gradient spectrum. (b) Temperature gradient spectrum (black), fitted Batchelor spectrum (dark grey), and the model noise spectrum of the FP07 sensor (light grey). (c) Stacked histogram of the background-corrected dissipation rates ($\varepsilon_{ml} - \varepsilon_{bulk}$) for the 41 measurements in August 2014 (blue), the 39 measurements in August 2015 (green), and the 23 measurements in July 2016 (magenta). Dissipation rates extracted from the mixed layer of the numerical simulation (at t = 10 h) are superimposed in black, and the counts are scaled to match the Lake Cadagno data.

Kamykowski et al., 1992] observed in the Krka Estuary, Croatia, and $R \approx 14 \times 10^{-10}$ W kg^{-1} for a population of the raphidophyte *Heterosigma akashiwo* [*Khan et al.*, 1997; *Sengupta et al.*, 2017; *Thompson et al.*, 1991; *Wada et al.*, 1985], reported from Kagoshima Bay, Japan (Table S1). Both populations were considered harmful algal blooms.

4. Conclusions and Discussion

We documented the first observation of bioconvection, in our case bacteria driven, within a natural water body by combining fieldwork, laboratory experiments and numerical simulations. A 0.3 to 1.2 m thick mixed layer of uniform temperature and salinity was observed to develop regularly during the summer months in Lake Cadagno at around 12 m depth, which coincided with the layer of maximum abundance of *C. okenii*. Using direct numerical simulations based on conditions found in Lake Cadagno, we showed that *C. okenii* are able to cause the observed mixed layer. Furthermore, the energy input rates of *C. okenii* estimated from the simulation agreed with turbulence measurements in Lake Cadagno.

Whether bioconvection has ecological significance is an open question [*Jánosi et al.*, 2002]. Bioconvective organisms may benefit from bioconvection by vertically expanding their habitat, by an increased transport of nutrients into the bioconvective layer, and by shuttling between vertically separated resource zones in bioconvective plumes. In August 2014 and July 2016, bioconvection in Lake Cadagno was more active with larger *C. okenii* concentrations, thicker mixed layers, and enhanced dissipation rates compared to August 2015 (Table 1). In these summer seasons of more active bioconvection, the ratio of *C. okenii* cells over the total cell number was enhanced (Table 1). This observation may indicate a beneficial effect of bioconvection for *C. okenii*.

Given our observations of bacteria-induced mixing in a natural water body and the wide range of species that form layers and are potentially capable of triggering bioconvection, we suggest that bioconvection is a natural and widespread phenomenon in water bodies of weak background turbulence. Our observations represent a reference case to which future observations can be compared. At the same time, our measurements provide realistic boundary conditions for future numerical simulations and laboratory studies that may shed more light on the ecological relevance of bioconvection.

Acknowledgments

We thank the personnel of Piora Centro Biologia Alpina for making it possible to use the laboratory facilities and housing; our technical staff Michael Schurter, Michael Plüss, Karin Beck, Patrick Kathriner, Christian Dinkel, and Serge Robert for support during field work and design of sampling devices; Samuel Lüdin, Patrick Stücheli, Jessica Zanetti, Jonathan Schenk, and Oliver Truffer for assisting during field work; Barry Ruddick and Jeffrey Carpenter for providing code for Batchelor fitting; Rosi Siber for the map used in Figure 1b; Kurt Hanselmann for discussions on the metabolism of *C. okenii*; Roman Stocker for comments on an early version of the manuscript and Prof. Kantha and one anonymous reviewer for constructive comments on the manuscript. This work was financed by Eawag, the ENAC Professors Visiting Program at EPFL, and the Swiss National Science Foundation Sinergia grant CRSII2_160726 (A Flexible Underwater Distributed Robotic System for High-Resolution Sensing of Aquatic Ecosystems). A.S. was supported by a Human Frontier Science Program (Cross Disciplinary Fellowship, LT000993/2014-C). There are no financial conflicts of interests for any author. The data from field measurements are available by contacting T. Sommer at tobias.sommer@hslu.ch. The simulation data from this paper are available by contacting G. Constantinescu at sconstan@engineering.uiowa.edu.

References

Batchelor, G. K. (1959), Small-scale variation of convected quantities like temperature in turbulent fluid. Part 1. General discussion and the case of small conductivity, *J. Fluid Mech.*, *5*(1), 113–133, doi:10.1017/S002211205900009X.

Bearon, R. N., and D. Grünbaum (2006), Bioconvection in a stratified environment: Experiments and theory, *Phys. Fluids*, *18*(12), 127102, doi:10.1063/1.2402490.

Borden, Z., E. Meiburg, and G. Constantinescu (2012), Internal bores: An improved model via a detailed analysis of the energy budget, *J. Fluid Mech.*, *703*, 279–314, doi:10.1017/jfm.2012.213.
Casamayor, E. O., I. Ferrera, X. Cristina, C. M. Borrego, and J. M. Gasol (2007), Flow cytometric identification and enumeration of photosynthetic sulfur bacteria and potential for ecophysiological studies at the single-cell level, *Environ. Microbiol.*, *9*(8), 1969–1985, doi:10.1111/j.1462-2920.2007.01313.x.
Chang, K., G. Constantinescu, and S. O. Park (2006), Analysis of the flow and mass transfer processes for the incompressible flow past an open cavity with a laminar and a fully turbulent incoming boundary layer, *J. Fluid Mech.*, *561*(2006), 113, doi:10.1017/S0022112006000735.
Cline, J. D. (1969), Spectrophotometric determination of hydrogen sulfide in natural waters, *Limnol. Oceanogr.*, *14*(3), 454–458, doi:10.4319/lo.1969.14.3.0454.
Del Don, C., K. W. Hanselmann, R. Peduzzi, and R. Bachofen (2001), The meromictic alpine Lake Cadagno: Orographical and biogeochemical description, *Aquat. Sci.*, *63*(1), 70–90, doi:10.1007/PL00001345.
Durham, W. M., and R. Stocker (2012), Thin phytoplankton layers: Characteristics, mechanisms, and consequences, *Annu. Rev. Mar. Sci.*, *4*(1), 177–207, doi:10.1146/annurev-marine-120710-100957.
Fenchel, T., and B. Finlay (2008), Oxygen and the spatial structure of microbial communities, *Biol. Rev.*, *83*(4), 553–569, doi:10.1111/j.1469-185X.2008.00054.x.
Gervais, F. (1997), Diel vertical migration of Cryptomonas and Chromatium in the deep chlorophyll maximum of a eutrophic lake, *J. Plankton Res.*, *19*(5), 533–550, doi:10.1093/plankt/19.5.533.
Gibson, C. H., and W. H. Schwarz (1963), The universal equilibrium spectra of turbulent velocity and scalar fields, *J. Fluid Mech.*, *16*, 365–384, doi:10.1017/S0022112063000835.
Gregg, M. C., and J. K. Horne (2009), Turbulence, acoustic backscatter, and pelagic nekton in Monterey Bay, *J. Phys. Oceanogr.*, *39*(5), 1097–1114, doi:10.1175/2008JPO4033.1.
Guerrero, R., C. Pedrós-Alió, T. M. Schmidt, and J. Mas (1985), A survey of buoyant density of microorganisms in pure cultures and natural samples, *Microbiologia*, *1*(1–2), 53–65.
Hieronymus, M., and J. R. Carpenter (2016), Energy and variance budgets of a diffusive staircase with implications for heat flux scaling, *J. Phys. Oceanogr.*, *46*(8), 2553–2569, doi:10.1175/JPO-D-15-0155.1.
Hill, N. A., and T. J. Pedley (2005), Bioconvection, *Fluid Dyn. Res.*, *37*(1–2), 1–20, doi:10.1016/j.fluiddyn.2005.03.002.
Imhoff, J. F. (2006), The Chromatiaceae, in *The Prokaryotes*, pp. 846–873, Springer, New York.
Jánosi, I. M., A. Czirók, D. Silhavy, and A. Holczinger (2002), Is bioconvection enhancing bacterial growth in quiescent environments? *Environ. Microbiol.*, *4*(9), 525–531.
Jékely, G. (2009), Evolution of phototaxis, *Philos. Trans. R. Soc. Lond. Ser. B Biol. Sci.*, *364*(1531), 2795–2808, doi:10.1098/rstb.2009.0072.
Jorgensen, B. B., J. G. Kuenen, and Y. Cohen (1979), Microbial transformations of sulfur compounds in a stratified lake (Solar Lake, Sinai), *Limnol. Oceanogr.*, *24*(5), 799–822, doi:10.4319/lo.1979.24.5.0799.
Kamykowski, D., R. E. Reed, and G. J. Kirkpatrick (1992), Comparison of sinking velocity, swimming velocity, rotation and path characteristics among six marine dinoflagellate species, *Mar. Biol.*, *113*, 319–328, doi:10.1007/BF00347287.
Katija, K. (2012), Biogenic inputs to ocean mixing, *J. Exp. Biol.*, *215*(6), 1040–1049, doi:10.1242/jeb.059279.
Katija, K., and J. O. Dabiri (2009), A viscosity-enhanced mechanism for biogenic ocean mixing, *Nature*, *460*(7255), 624–626, doi:10.1038/nature08207.
Kessler, J. O. (1986), Individual and collective fluid dynamics of swimming cells, *J. Fluid Mech.*, *173*(1), 191, doi:10.1017/S0022112086001131.
Khan, S., O. Arakawa, and Y. Onoue (1997), Neurotoxins in a toxic red tide of *Heterosigma akashiwo* (Raphidophyceae) in Kagoshima Bay, Japan, *Aquac. Res.*, *28*, 9–14, doi:10.1111/j.1365-2109.1997.tb01309.x.
Kils, U. (1993), Formation of micropatches by zooplankton-driven microturbulences, *Bull. Mar. Sci.*, *53*(1), 160–169.
Kim, Y.-C. (1996), Diffusivity of bacteria, *Korean J. Chem. Eng.*, *13*(3), 282–287, doi:10.1007/BF02705951.
Kunze, E. (2011), Fluid mixing by swimming organisms in the low-Reynolds-number limit, *J. Mar. Res.*, *69*(4), 591–601, doi:10.1357/002224011799849435.
Kunze, E., J. F. Dower, I. Beveridge, R. Dewey, and K. P. Bartlett (2006), Observations of biologically generated turbulence in a coastal inlet, *Science*, *313*(5794), 1768–1770, doi:10.1126/science.1129378.
Lebert, M., and D. P. Hader (1996), How *Euglena* tells up from down, *Nature*, *379*, 590, doi:10.1038/379590a0.
Legović, T., D. Viličić, D. Petricioli, and V. Žutić (1991), Subsurface *Gonyaulax polyedra* bloom in a stratified estuary, *Mar. Chem.*, *32*(2–4), 361–374, doi:10.1016/0304-4203(91)90049-3.
Musat, N., H. Halm, B. Winterholler, P. Hoppe, S. Peduzzi, F. Hillion, F. Horreard, R. Amann, B. B. Jørgensen, and M. M. M. Kuypers (2008), A single-cell view on the ecophysiology of anaerobic phototrophic bacteria, *Proc. Natl. Acad. Sci. U.S.A.*, *105*(46), 17,861–17,866, doi:10.1073/pnas.0809329105.
Ooi, S. K., G. Constantinescu, and L. Weber (2009), Numerical simulations of lock-exchange compositional gravity current, *J. Fluid Mech.*, *635*(2009), 361–388, doi:10.1017/S0022112009007599.
Pedley, T. J., and J. O. Kessler (1992a), Bioconvection, *Sci. Prog.*, *76*(1), 105–123.
Pedley, T. J., and J. O. Kessler (1992b), Hydrodynamic phenomena in suspensions of swimming microorganisms, *Annu. Rev. Fluid Mech.*, *24*(1), 313–358, doi:10.1146/annurev.fluid.24.1.313.
Pfennig, N. (1962), Beobachtungen über das Schwaermen von *Chromatium okenii*, *Arch. Mikrobiol.*, *42*(1), 90–95, doi:10.1007/BF00425194.
Pierce, C. D., and P. Moin (2004), Progress-variable approach for large-eddy simulation of non-premixed turbulent combustion, *J. Fluid Mech.*, *504*(3), 73–97, doi:10.1017/S0022112004008213.
Ruddick, B., A. Anis, and K. Thompson (2000), Maximum likelihood spectral fitting: The Batchelor spectrum, *J. Atmos. Ocean. Technol.*, *17*(11), 1541–1555, doi:10.1175/1520-0426(2000)017<1541:MLSFTB>2.0.CO;2.
Sengupta, A., F. Carrara, and R. Stocker (2017), Phytoplankton can actively diversify their migration strategy in response to turbulent cues, *Nature*, *543*(7646), 555–558, doi:10.1038/nature21415.
Smayda, T. J. (2010), Adaptations and selection of harmful and other dinoflagellate species in upwelling systems. 2. Motility and migratory behaviour, *Prog. Oceanogr.*, *85*(1–2), 71–91, doi:10.1016/j.pocean.2010.02.005.
Sommer, T., J. R. Carpenter, M. Schmid, R. G. Lueck, and A. Wüest (2013), Revisiting microstructure sensor responses with implications for double-diffusive fluxes, *J. Atmos. Ocean. Technol.*, *30*(8), 1907–1923, doi:10.1175/JTECH-D-12-00272.1.
Steinbuck, J. V., M. T. Stacey, and S. G. Monismith (2009b), An evaluation of χ_T estimation techniques: Implications for Batchelor fitting and ε, *J. Atmos. Ocean. Technol.*, *26*(8), 1652–1662, doi:10.1175/2009JTECHO611.1.
Thompson, P. A., P. J. Harrison, and J. S. Parslow (1991), Influence of irradiance on cell volume and carbon quota for ten species of marine phytoplankton, *J. Phycol.*, *27*, 351–360, doi:10.1111/j.0022-3646.1991.00351.x.

Tonolla, M., R. Peduzzi, and D. Hahn (2005), Long-term population dynamics of phototrophic sulfur bacteria in the chemocline of Lake Cadagno, Switzerland, *Appl. Environ. Microbiol.*, *71*(7), 3544–3550, doi:10.1128/AEM.71.7.3544-3550.2005.

Vaituzis, Z., and R. N. Doetsch (1969), Motility tracks: Technique for quantitative study of bacterial movement, *Appl. Microbiol.*, *17*(4), 584–588.

Visser, A. W. (2007), Biomixing of the oceans?, *Science*, *316*(5826), 838–839, doi:10.1126/science.1141272.

Wada, M., A. Miyazaki, and T. Fujii (1985), On the mechanisms of diurnal vertical migration behavior of *Heterosigma akashiwo* (Raphidophyceae), *Plant Cell Physiol.*, *26*, 431–436.

Winters, K. B., P. N. Lombard, J. J. Riley, and E. A. D'Asaro (1995), Available potential energy and mixing in density-stratified fluids, *J. Fluid Mech.*, *289*, 115–128, doi:10.1017/S002211209500125X.

Wüest, A. (1994), Interactions in lakes: Biology as source of dominant physical forces, *Limnologica*, *24*(2), 93–104.

Wüest, A., G. Piepke, and J. D. Halfman (1996), Combined effects of dissolved solids and temperature on the density stratification of Lake Malawi, in *The Limnology, Climatology and Paleoclimatology of the East African Lakes*, edited by T. C. Johnson and E. O. Odada, pp. 183–202, Gordon and Breach, New York.